Materials Physics and Mechanics 42 (2019) 340-350 Received: January 16, 2019

FINITE ELEMENT MODELING AND INVESTIGATION OF ELASTIC HOMOGENEOUS AND HETEROGENEOUS MATERIALS

V.L. Leontiev[1*], I.V. Efremenkov[2]

[1]Peter the Great St. Petersburg Polytechnic University (SPbPU),

Polytechnicheskaya st., 29, Saint Petersburg 195251, Russia

[2]Ulyanovsk State University, L. Tolstoy st., 42. Ulyanovsk, 432000, Russia

*e-mail: leontiev_vl@spbstu.ru

Abstract. A novel finite element (FE) connected with orthogonal finite functions (OFF) was developed for ANSYS software and was tested. The FE is proposed for modeling and investigation of stress-strain states of homogeneous and heterogeneous elastic materials. The efficiency of the developed FE is demonstrated using the examples of plane problems of elasticity. The accuracy of this FE was found to be higher than that of the classical FE of ANSYS. Moreover, the developed FE was proved to require less computational time, and this difference in computational time increases with the increasing number of FE in the model.
Keywords: homogeneous and heterogeneous materials, finite element methods, orthogonal finite functions, shape functions

1. Introduction

Finite element simulations and investigations of stress-strain states of technical constructions often require very fine meshes. Even when supercomputers are used, the advantages of numerical methods are usually taken into account because in that case methods with high accuracy and low computational time allow investigation of constructions' stress-strain states without almost any geometrical simplifications. Therefore, the development of advanced discrete models and numerical methods can be referred to as an actual direction in computational mechanics.

It is impossible [1] to create basis OFFs by the classical procedure of orthogonalization of the splines. The first OFFs, Daubechies's compactly supported orthonormal wavelets [2], do not have an analytical form, and their smoothness is very low. They are also characterized by poor efficiency in numerical methods. The OFFs [3] were created by the author of this paper specifically for their application in numerical methods without the classical procedure of orthogonalization. The structure of some OFFs is presented here, and the novel FE for the ANSYS software is constructed on the basis of these OFFs. The corresponding discrete modeling of homogeneous and heterogeneous elastic plates was made. The series of approximate solutions for the plane problem were obtained and analyzed. This analysis shows that the application of the OFFs in the FE provides an increase in accuracy of approximate solutions in comparison with the classical FE. Besides, the solution requires much less computational time.

Mixed finite elements are well known, but classical mixed FEs [4-9] have a strong disadvantage – the number of unknown variables at each node is significantly higher than that in the case of FE connected with the Lagrange's variational principle. Orthogonal finite functions [3] provide possibilities for exception of a part of unknown values at grid nodes

http://dx.doi.org/10.18720/MPM.4232019_9

(stresses, strains) prior to the solution of FE systems formulated using mixed numerical methods. The fundamental properties of the basic functions (functions are compactly supported – finite functions) of numerical methods are retained in that case. Thereby, the OFFs [3] remove the mentioned disadvantage of mixed numerical methods. Mixed FEs allow obtaining approximate solutions for derivatives (strains and stresses) of the main unknown function (displacement) without numerical differentiation, because the derivatives are approximated independently [3,4-9]. Consequently, the approximate solutions [3,4-9] for derivatives (strains and stresses) have accuracy and smoothness same as those of solutions for displacement. The computational time of the mixed FEMs [3] is less than that of classical mixed FEMs [4-9]. The computational time of mixed FEMs [3] is approximately equal to the computational time of classical FEMs connected with the Lagrange's variational principle.

ANSYS allows creating a new FE by means of linking an additional dynamical Fortran library. Here, on the examples of plane problems of elasticity, it is shown for the FEM of ANSYS connected with the Lagrange's variational principle that application of OFFs also increases the accuracy of approximate solutions "in displacements" and simultaneously decreases the computational time significantly due to increase in the number of zero elements in global FE matrixes. Application of OFFs in 3D FE for elasticity gives similar results**:** high accuracy of approximate solutions and even more significant difference in computational time between the novel FEM (OFF) and the classic FE of ANSYS. These results are the content of the next article. Application area of the novel FE for plane problems of elasticity comprises problems of mechanics of deformable heterogeneous bodies. The FE allows obtaining approximate solutions for analysis of stress-strain states of heterogeneous bodies with significantly smaller computational time and with higher accuracy. Simplification of the construction structure by elimination of numerous small features becomes unnecessary in that case.

The base finite function [3]

$$\varphi^{(1)}(x)=\begin{cases} 1+x, x\in[-1,-1+H_1]\cup[-1+H_2,0], \\ -\alpha+2(\alpha+H_1)(K_N-1-x)/H_2-H_1, x\in[-1+H_1,-1+K_N], \\ -\alpha+2(\alpha+H_2)(1-K_N+x)/H_2-H_1, x\in[-1+K_N,-1+H_2], \\ 1-x, x\in[0,H_1]\cup[H_2,1], \\ \beta+2(\beta+H_1-1)(x-K_N)/H_2-H_1, x\in[H_1,K_N], \\ \beta+2(\beta+H_2-1)(K_N-x)/H_2-H_1, x\in[K_N,H_2], \\ 0, x\notin[-1,1], \end{cases} \quad (1)$$

where $K_N=(H_1+H_2)/2, \alpha>0, \beta>0$; generates finite functions on the grid. The function (1) is the sum of the even functions – the B-spline of first degree which has the compact support [-1, 1] and two B-splines of first degree with smaller compact supports. The uniform grid $a=x_1<x_2<\cdots<x_N=b$ is used (h – the step of the grid). Then the function (1) generates the grid finite functions

$$\varphi_i(x)=\varphi^{(1)}(x/h-i)=$$

$$=\begin{cases} (x-x_{i-1})/h, x\in[x_{i-1},x_{i-1}+h_1]\cup[x_{i-1}+h_2,x_i], \\ -\alpha+2(\alpha h+h_1)(x_{i-1}+k_N-x)/)), x\in[x_{i-1}+h_1,x_{i-1}+k_N], \\ -\alpha+2(\alpha h+h_2)(x-x_{i-1}-k_N)/(h(h_2-h_1)), x\in[x_{i-1}+k_N,x_{i-1}+h_2], \\ (x_{i+1}-x)/h, x\in[x_i,x_i+h_1]\cup[x_i+h_2,x_{i+1}], \\ \beta+2(\beta h+h_1-h)(x-x_i-k_N)/(h(h_2-h_1)), x\in[x_i+h_1,x_i+k_N], \\ \beta+2(\beta h+h_2-h)(x_i+k_N-x)/(h(h_2-h_1)), x\in[x_i+k_N,x_i+h_2], \\ 0, x\notin[x_{i-1},x_{i+1}], \end{cases} \quad (2)$$

where $k_N = h_1 + h_2/2, h_1 = H_1 h, h_2 = H_2 h$ $(0 \le h_1 < h_2 \le h)$. Grids for OFFs can be non-uniform. The theorem [3] about approximate properties of a sequence of groups of the functions (2) on grids has been proved for the Sobolev's space. The condition [3] connects the free parameters (2) and defines their values for which the functions (2) are orthogonal on the grid. This property is valuable for algorithms of numerical methods. The main properties of basis functions of numerical methods (functions are compactly supported – finite functions) are remained and that improves the characteristics of the global FE matrix.

2. The finite element connected with OFFs

The novel FE, which is similar to the FE Plane142 of ANSYS, is being constructed. The local stiffness matrix, the vector of body forces and loads on a boundary are created for the quadrangular FE. The nodes of the base FE are assumed to have the following numbers and coordinates**:**1(-1,-1), 2(1,-1), 3(1,1), 4(-1,1).

The system of equations of a plane problem of elasticity can be written in a matrix form:

$$\varepsilon = Bu,\ \sigma = D\varepsilon,\ B^T\sigma = f, \tag{3}$$

where $u = (u_x, u_y)^T$ – the displacement vector; $\varepsilon = (\varepsilon_{xx}, \varepsilon_{yy}, \varepsilon_{xy})^T$ – the strain vector; $\sigma = (\sigma_{xx}, \sigma_{yy}, \sigma_{xy})^T$ – the stress vector; D – the symmetric matrix of elastic modules (has different components for "plain stress" and "plain strain" problems); B – the matrix differential operator; $f = (f_x, f_y)^T$ – the vector of body forces.

The approximations of components of the displacement vector have forms [10]

$$u_x(x,y) = \sum_{i=1}^{n_p} N_i(x,y)u_i, \quad u_y(x,y) = \sum_{i=1}^{n_p} N_i(x,y)v_i, \tag{4}$$

where u_i, v_i – unknown constant coefficients; n_p – the number of nodes of a grid; $N_i(x,y)$ - the shape functions which form a Lagrange's basis on the grid:

$$N_i(x_j, y_j) = \delta_{ij},\ \delta_{ij} = \begin{cases} 1, i = j; \\ 0, i \ne j \end{cases}$$

The problem (3) after the discretization (4) and after the exception of ε and σ is written as

$$Ku = f,\ K = \sum_{(e)} k^{(e)},\ f = \sum_{(e)} f^{(e)},$$

where

$$k^{(e)} = \int_{S^{(e)}} B^T DB dS,\ f^{(e)} = \int_{S^{(e)}} N^T f dS + \int_{l^{(e)}} N^T p dl \tag{5}$$

are accordingly a local stiffness matrix and a local vector of body forces and loads on the boundary for the FE $S^{(e)}$ ($p = (p_x, p_y)^T$ is a vector of a load on the boundary $l^{(e)}$ of the region $S^{(e)}$).

Structures of the classic local stiffness matrix (5) and the local vector of body forces and loads on the boundary (5) are described further for a classic bilinear quadrangular FE. These structures define also the subprograms for the novel FE, which is connected with OFFs.

The Gauss's formula was used for calculation of the integrals (5). The Gauss's points were generated, the nodes $t_1, t_2, ..., t_s$ and the coefficients $W_1, W_2, ..., W_s$ were taken so that the Gauss's formula

$$\int_{-1}^{1} f(x)dx \cong \sum_{i=1}^{s} W_i f(t_i)$$

is exact for all polynomials of the degree $(2s-1)$. The local stiffness matrix of the bilinear quadrangular FE is written for s=2 as

$$k^{(e)} = \int_{S^{(e)}} B_N^T D B_N dS = \sum_{i=1}^{2}\sum_{j=1}^{2} W_i W_j B_N^T(\xi_i,\eta_j) D B_N(\xi_i,\eta_j) det\left|J(\xi_i,\eta_j)\right|, \quad (6)$$

where

$$B_N = B \cdot N^T = \begin{pmatrix} \frac{\partial}{\partial x} & 0 \\ 0 & \frac{\partial}{\partial y} \\ \frac{\partial}{\partial y} & \frac{\partial}{\partial x} \end{pmatrix} \begin{pmatrix} N_1 & 0 & N_2 & 0 & N_3 & 0 & N_4 & 0 \\ 0 & N_1 & 0 & N_2 & 0 & N_3 & 0 & N_4 \end{pmatrix} =$$

$$= \begin{pmatrix} \frac{\partial N_1}{\partial x} & 0 & \frac{\partial N_2}{\partial x} & 0 & \frac{\partial N_3}{\partial x} & 0 & \frac{\partial N_4}{\partial x} & 0 \\ 0 & \frac{\partial N_1}{\partial y} & 0 & \frac{\partial N_2}{\partial y} & 0 & \frac{\partial N_3}{\partial y} & 0 & \frac{\partial N_4}{\partial y} \\ \frac{\partial N_1}{\partial y} & \frac{\partial N_1}{\partial x} & \frac{\partial N_2}{\partial y} & \frac{\partial N_2}{\partial x} & \frac{\partial N_3}{\partial y} & \frac{\partial N_3}{\partial x} & \frac{\partial N_4}{\partial y} & \frac{\partial N_4}{\partial x} \end{pmatrix},$$

the derivatives of the shape functions N_i in the global (x, y) and in local (ξ,η) coordinate systems are connected by the Jacobi's matrix J.

The algorithm of calculation of the first integral in the right part of the second formula (5) is similar to (6), but for the second integral it is necessary to make an additional explanation. That can be illustrated on the example of the part of the FE boundary with nodes 2(1,-1) and 3(1,1) and the local coordinate $\xi = 1$. For this part of the boundary, the classical shape functions have the forms:

$$N_1 = \frac{(1-\xi)(1-\eta)}{4} = 0, \qquad N_2 = \frac{(1+\xi)(1-\eta)}{4} = \frac{1-\eta}{2},$$

$$N_3 = \frac{(1+\xi)(1+\eta)}{4} = \frac{1+\eta}{2}, \qquad N_4 = \frac{(1-\xi)(1+\eta)}{4} = 0,$$

consequently, in the case of a constant load on the boundary

$$\int_{l^{(e)}} N^T p dl = l^{(e)} \int_{-1}^{1} N^T \cdot p d\eta =$$

$$= \frac{l^{(e)}}{2} \int_{-1}^{1} \begin{pmatrix} 0 & 0 & (1-\eta) & 0 & (1+\eta) & 0 & 0 & 0 \\ 0 & 0 & 0 & (1-\eta) & 0 & (1+\eta) & 0 & 0 \end{pmatrix}^T \cdot \begin{pmatrix} p_x \\ p_y \end{pmatrix} d\eta =$$

$$= l^{(e)} \begin{pmatrix} 0 & 0 & p_x & p_y & p_x & p_y & 0 & 0 \end{pmatrix}^T.$$

The creation of the novel FE of ANSYS on the base of OFFs is similar to the creation of the classic FE of ANSYS. The structure of the subprogram UserElem.f of ANSYS was used for that. This structure defines the variables, the functions, the computations of derivatives of

shape functions, the construction of the Jacobi's matrix, the creation of local and global stiffness matrices, verifications, and output of results.

The grid functions

$$\varphi_i(x)=\begin{cases}\dfrac{(\sqrt{2}-1)(x_{i-1}-x)}{h_{i-1}},\ x\in\left[x_{i-1},x_{i-1}+\dfrac{h_{i-1}}{2}\right];\\ \dfrac{(\sqrt{2}+1)(x-x_i)}{h_{i-1}}+1,\ x\in\left[x_{i-1}+\dfrac{h_{i-1}}{2},x_i\right];\\ \dfrac{(\sqrt{2}-1)(x-x_i)}{h_i}+1,\ x\in\left[x_i,x_i+\dfrac{h_i}{2}\right];\\ \dfrac{(\sqrt{2}+1)(x_{i+1}-x)}{h_i},\ x\in\left[x_i+\dfrac{h_i}{2},x_{i+1}\right];\\ 0,\ x\notin[x_{i-1},x_{i+1}]\end{cases}$$

follow from (2) and for the given values of parameters are orthogonal on non-uniform grids.

The shape functions for the novel bilinear quadrangular FE are the tensor products of single-argument OFFs

$$N_i=\varphi_i(\xi)\varphi_i(\eta),\quad i=\overline{1,4}\,; \tag{7}$$

and are defined in local coordinates by Table 1.

Table 1. OFFs for the shape functions (7)

	$\varphi_i(\xi)$	$\varphi_i(\eta)$
N_1	$\begin{cases}\dfrac{(\sqrt{2}-1)(\xi+1)}{2}+1,\ \xi\in[-1,0]\\ \dfrac{(\sqrt{2}+1)(1-\xi)}{2},\ \xi\in[0,1]\end{cases}$	$\begin{cases}\dfrac{(\sqrt{2}-1)(\eta+1)}{2}+1,\ \eta\in[-1,0]\\ \dfrac{(\sqrt{2}+1)(1-\eta)}{2},\ \eta\in[0,1]\end{cases}$
N_2	$\begin{cases}\dfrac{(\sqrt{2}-1)(-1-\xi)}{2},\ \xi\in[-1,0]\\ \dfrac{(\sqrt{2}+1)(\xi-1)}{2}+1,\ \xi\in[0,1]\end{cases}$	$\begin{cases}\dfrac{(\sqrt{2}-1)(\eta+1)}{2}+1,\ \eta\in[-1,0]\\ \dfrac{(\sqrt{2}+1)(1-\eta)}{2},\ \eta\in[0,1]\end{cases}$
N_3	$\begin{cases}\dfrac{(\sqrt{2}-1)(-1-\xi)}{2},\ \xi\in[-1,0]\\ \dfrac{(\sqrt{2}+1)(\xi-1)}{2}+1,\ \xi\in[0,1]\end{cases}$	$\begin{cases}\dfrac{(\sqrt{2}-1)(-1-\eta)}{2},\ \eta\in[-1,0]\\ \dfrac{(\sqrt{2}+1)(\eta-1)}{2}+1,\ \eta\in[0,1]\end{cases}$
N_4	$\begin{cases}\dfrac{(\sqrt{2}-1)(\xi+1)}{2}+1,\ \xi\in[-1,0]\\ \dfrac{(\sqrt{2}+1)(1-\xi)}{2},\ \xi\in[0,1]\end{cases}$	$\begin{cases}\dfrac{(\sqrt{2}-1)(-1-\eta)}{2},\ \eta\in[-1,0]\\ \dfrac{(\sqrt{2}+1)(\eta-1)}{2}+1,\ \eta\in[0,1]\end{cases}$

The subprogram for computation of values of the shape functions (7) is constructed by use of FORTRAN 77 programming language.

Let the variables ft and fs correspond to the basis functions $\varphi_i(\xi)$ and $\varphi_i(\eta)$, and *intPnt* be the number of nodes of the FE, then Part 1 of the subprogram for the shape functions (7) has the following form:

Part 1 of the subprogram

```
if (intPnt.EQ.1) then
        ft(1)=((((sqrt(2.)-1.)*(-Pnt(1,1)+1.))/2.)+1.)
        ft(2)=((((sqrt(2.)-1.)*(-1.+Pnt(1,2)))/2.))
        ft(3)=((((sqrt(2.)-1.)*(-1.+Pnt(1,3)))/2.))
        ft(4)=((((sqrt(2.)-1.)*(-Pnt(1,4)+1.))/2.)+1.)
        fs(1)=((((sqrt(2.)-1.)*(-Pnt(2,1)+1.))/2.)+1.)
        fs(2)=((((sqrt(2.)-1.)*(-Pnt(2,2)+1.))/2.)+1.)
        fs(3)=((((sqrt(2.)-1.)*(-1.+Pnt(2,3)))/2.))
        fs(4)=((((sqrt(2.)-1.)*(-1.+Pnt(2,4)))/2.))
end if
if (intPnt.EQ.2) then
        ft(1)=((((sqrt(2.)+1.)*(1.-Pnt(1,1)))/2.))
        ft(2)=((((sqrt(2.)+1.)*(Pnt(1,2)-1.))/2.)+1.)
        ft(3)=((((sqrt(2.)+1.)*(Pnt(1,3)+1.))/2.)+1.)
        ft(4)=((((sqrt(2.)+1.)*(1.-Pnt(1,4)))/2.))
        fs(1)=((((sqrt(2.)-1.)*(-Pnt(2,1)+1.))/2.)+1.)
        fs(2)=((((sqrt(2.)-1.)*(-Pnt(2,2)+1.))/2.)+1.)
        fs(3)=((((sqrt(2.)-1.)*(-1.+Pnt(2,3)))/2.))
        fs(4)=((((sqrt(2.)-1.)*(-1.+Pnt(2,4)))/2.))
end if
if (intPnt.EQ.3) then
        ft(1)=((((sqrt(2.)+1.)*(1.-Pnt(1,1)))/2.))
        ft(2)=((((sqrt(2.)+1.)*(Pnt(1,2)-1.))/2.)+1.)
        ft(3)=((((sqrt(2.)+1.)*(Pnt(1,3)+1.))/2.)+1.)
        ft(4)=((((sqrt(2.)+1.)*(1.-Pnt(1,4)))/2.))
        fs(1)=((((sqrt(2.)+1.)*(1.-Pnt(2,1)))/2.))
        fs(2)=((((sqrt(2.)+1.)*(1.-Pnt(2,2)))/2.))
        fs(3)=((((sqrt(2.)+1.)*(Pnt(2,3)-1.))/2.)+1.)
        fs(4)=((((sqrt(2.)+1.)*(Pnt(2,4)-1.))/2.)+1.)
end if
if (intPnt.EQ.4) then
        ft(1)=((((sqrt(2.)-1.)*(-Pnt(1,1)+1.))/2.)+1.)
        ft(2)=((((sqrt(2.)-1.)*(-1.+Pnt(1,2)))/2.))
        ft(3)=((((sqrt(2.)-1.)*(-1.+Pnt(1,3)))/2.))
        ft(4)=((((sqrt(2.)-1.)*(-Pnt(1,4)+1.))/2.)+1.)
        fs(1)=((((sqrt(2.)+1.)*(1.-Pnt(2,1)))/2.))
        fs(2)=((((sqrt(2.)+1.)*(1.-Pnt(2,2)))/2.))
        fs(3)=((((sqrt(2.)+1.)*(Pnt(2,3)-1.))/2.)+1.)
        fs(4)=((((sqrt(2.)+1.)*(Pnt(2,4)-1.))/2.)+1.)
end if
```

The cycle operator was used for the computation of values of the shape functions (7) in the nodes of the FE. Let $Nn\ (i),\ (i = \overline{1..4})$ be an array of values of the shape functions (7) at all nodes of the FE. Part 2 of the subprogram for this case is presented below.

The shape functions (7) are formed in the subprogram, and their values are transmitted to the system variables of the FE library. The local stiffness matrix and the local load vector were created similarly to such matrix and vector of the FE Plane142 of ANSYS. The novel FE was created in the FE library of ANSYS and was named as User300.

Part 2 of the subprogram

```
if (intPnt.EQ.1) then
 Nn(1)=ft(1)*fs(1)
 Nn(2)=(ft(2)*fs(2))
 Nn(3)=ft(3)*fs(3)
 Nn(4)=(fs(4)*ft(4))
end if
if (intPnt.EQ.2) then
 Nn(1)=ft(1)*fs(1)
 Nn(2)=ft(2)*fs(2)
 Nn(3)=ft(3)*fs(3)
 Nn(4)=ft(4)*fs(4)
end if
if (intPnt.EQ.3) then
 Nn(1)=ft(1)*fs(1)
 Nn(2)=ft(2)*fs(2)
 Nn(3)=ft(3)*fs(3)
 Nn(4)=ft(4)*fs(4)
end if
if (intPnt.EQ.4) then
 Nn(1)=ft(1)*fs(1)
 Nn(2)=ft(2)*fs(2)
 Nn(3)=ft(3)*fs(3)
 Nn(4)=ft(4)*fs(4)
end if
```

3. Solutions for the plane problems of elasticity for homogeneous and heterogeneous materials

Approximate solutions for several plane problems of elasticity were obtained and analyzed.

Problem 1. A homogeneous isotropic square plate is considered, the length of the side of the plate is equal to 2 *m*. The center of the plate coincides with the origin of coordinates. The modulus of elasticity is equal to 200 *GPa*, the Poisson's ratio is equal to 0.33. The side ($x=-1$) of the plate is fixed, and a uniform force $p_x=10$ *N* is applied to the opposite side ($x=1$); two sides ($y=-1$, $y=1$) of the plate are free (Fig. 1).

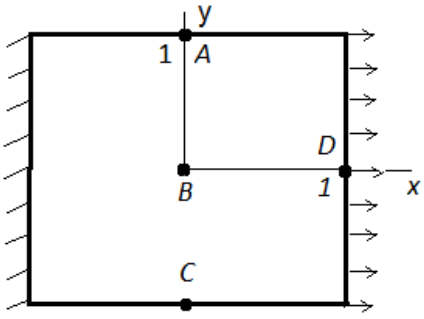

Fig. 1. The homogeneous square plate

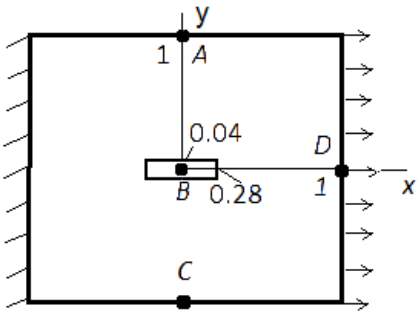

Fig. 2. The heterogeneous square plate

Series of computations were conducted for different numbers *M* of divisions along every side of the plate boundary, ranging from 10 to 100 (corresponds to the total number of FEs in the model ranging from 100 to 10000). Results of the computations are presented in Fig. 3 and in Tables 2-5 for the following points: points *A* (0, 1) and *C* (0, −1) are in the

middle of the opposite sides of the plate which are free (Fig. 1), point B (0, 0) is in the center of the plate, and point D is in the middle of the side on which the external load is applied.

The computational time [ms] of the methods that use User300 (t_1) or Plane142 (t_2) for the different numbers M, and the coefficient $k=t_2/t_1$ are presented in Table 2 and are shown in Fig. 3. The coefficient k is the ratio of computational time of two FEMs. It increases with rise of total number of FE due to the zero elements in the global grid matrix produced by OFFs. Thereby, the obtained results prove that the novel FE provides high accuracy of the approximate solutions at a relatively low computational time.

Table 2

M	t_1	t_2	k
10	0.000	0.000	0.00
20	0.010	0.006	0.60
30	0.040	0.062	1.55
40	0.120	0.125	1.04
50	0.062	0.125	2.02
60	0.094	0.219	2.33
70	0.172	0.266	1.55
80	0.188	0.312	1.66
90	0.250	0.562	2.25
100	0.266	0.622	2.34

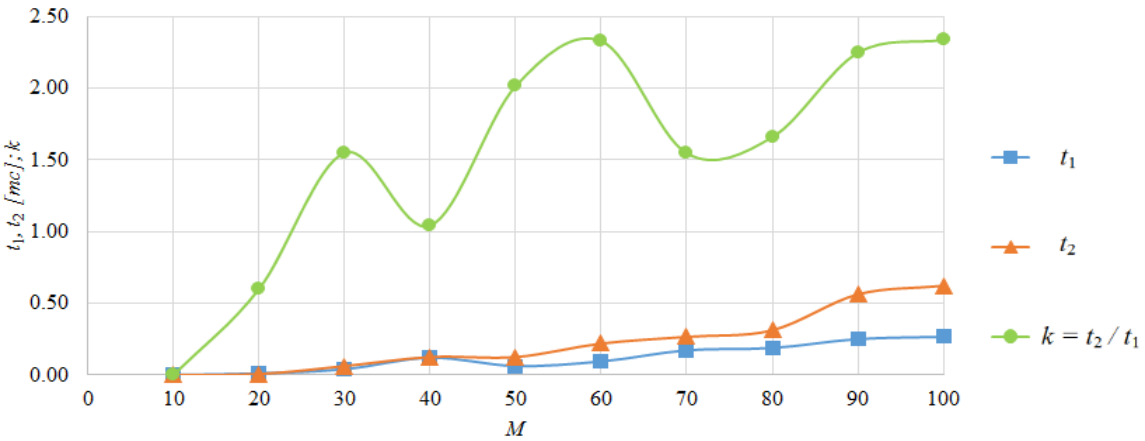

Fig. 3. The computational time and the coefficient k

Table 3

M	$10^9 U_{300}$ at point A	$10^9 U_{142}$ at point A	ε_1 at point A	ε_2 at point A
10	2.620063556	0.2914537501	798.963748142213	1.242032506472
20	2.623274810	0.5539481345	373.559643335165	1.120990817457
30	2.629161510	0.8163550033	222.061051793887	0.899103632349
40	2.635150100	1.078745142	144.279208999673	0.673375910899
50	2.644124400	1.341128972	97.156608738149	0.335107922839
60	2.650115000	1.603509427	65.269686312858	0.109304438525
66	2.650664780	1.760936616	50.525848342062	0.088581599477
70	2.651109410	1.865887724	42.083008312884	0.071822175841
76	2.651712470	2.023313942	31.057885529066	0.049091055545

80	2.652105320	2.128264497	24.613520722561	0.034283373708
86	2.652384210	2.285689993	16.043042500208	0.023771182318
90	2.652625110	2.390640126	10.958779665359	0.014690946720
96	2.652790241	2.548065063	4.109988379838	0.008466669491
100	2.652914453	2.653014863	0.003784750753	0.003784750753

Table 4

M	$10^9 U_{300}$ at point B	$10^9 U_{142}$ at point B	ε_1 at point B	ε_2 at point B
10	2.354386940	0.2530536263	830.390516201822	1.6634500738085
20	2.364379203	0.4911274176	381.418694674805	1.2460995301569
30	2.371358460	0.7290775710	225.254616836924	0.9545943222542
40	2.377346930	0.9669864625	145.851107765637	0.7044716813528
50	2.384330250	1.204875647	97.8901520614766	0.4127967726267
60	2.390327060	1.442753634	65.6781174324874	0.1623257918613
66	2.391776400	1.585476860	50.8553332024032	0.1017906721456
70	2.392956900	1.680624550	42.3849782510912	0.0524842921213
76	2.393279400	1.823344694	31.2576501785679	0.0390143153675
80	2.393484700	1.918490667	24.7587356649883	0.0304394743519
86	2.393581570	2.061208626	16.1251481197712	0.0263934692414
90	2.393666810	2.156353353	11.0053139792623	0.0228332186414
96	2.393899556	2.299069696	4.1247057522870	0.0131120303948
100	2.394299556	2.394213486	0.0035949175169	0.0035949175169

Table 5

M	$10^9 U_{300}$ at point D	$10^9 U_{142}$ at point D	ε_1 at point D	ε_2 at point D
10	4.840145745	0.5095828728	849.825043845155	1.748237213357
20	4.853458480	1.000479579	385.113197897665	1.477997482949
30	4.869125470	1.491258513	226.511160040566	1.159967930502
40	4.884046840	1.982001553	146.419930025151	0.857073971739
50	4.900145748	2.472727909	98.167607934739	0.530276769078
60	4.913012570	2.963444851	65.787211067624	0.269088778144
66	4.920997840	3.257872015	51.049452444497	0.106993069634
70	4.923254780	3.454155841	42.531345041302	0.061178677840
76	4.924048724	3.748580402	31.357692671414	0.045062138863
80	4.924617846	3.944862772	24.836227028077	0.033509338041
86	4.925134567	4.239285476	16.178412491511	0.023020242920
90	4.925547622	4.435566783	11.046634240249	0.014635499151
96	4.925885447	4.729988103	4.141603313458	0.007777874709
100	4.926427484	4.926268606	0.003225118497	0.003225118497

The values $(10^9 U_{300})$ $[m]$ and $(10^9 U_{142})$ $[m]$ of the displacement vector magnitude for selected points of the plate are presented in Tables 3-5. These displacements were received by two FEMs which are connected with User300 and Plane142 FEs. Tables 3-5 contain also: ε_1 [%] – a relative difference between the values of such two solutions obtained on the stated grid, and ε_2 [%] – a relative difference between the value of the User300 solution on the stated grid and the value of the Plane142 solution on the dense grid (M=100; 10000 FE). The solution obtained by use of Plane142 element on the dense grid is considered to be a reference solution for comparison with others, because an additional increase of the number of nodes of the grid gives only a variation of last ciphers of the mantissa.

A similar table for the point C coincides with the Table 3 and therefore is not provided. Tables 3-5 show a high accuracy of the approximate solutions obtained by the elements connected with OFF in comparison with those obtained by classical FEM of ANSYS, which is demonstrated by ε_1. The accuracy ε_2 of the approximate solutions obtained by use of the novel FEM (OFF) increases with the increase in the number of grids' cells.

Problem 2. A heterogeneous square plate has the same sizes and properties as considered in Problem 1, but a small rectangular region $(-0.28 \le x \le 0.28, -0.04 \le y \le 0.04)$ of the plate (Fig. 2) is assumed to be characterized by different material properties**:** the modulus of elasticity 160 GPa, and the Poisson's ratio 0.3. Boundary conditions are identical to those of Problem 1.

The results of computations are presented in Tables 6-8 show that the characteristics of approximate solutions for the heterogeneous plate (Problem 2) are similar to those of approximate solutions for the homogeneous plate (Problem 1). The FEM connected with OFF demonstrates a high accuracy of approximate solutions and reduced computational time in both Problems 1, 2. Thereby, this FEM and corresponding FE models are effective in the plane problems for elastic homogeneous and heterogeneous materials.

Table 6

M	$10^9 U_{300}$ in point A	$10^9 U_{142}$ in point A	ε_1 in point A	ε_2 in point A
50	2.647846135	1.344217665	96.9804596	0.427095692
60	2.652324564	1.636720729	62.05113781	0.258683251
70	2.656648790	1.894932755	40.19752326	0.096069672
80	2.657216879	2.183838367	21.67644454	0.074706547
90	2.658648790	2.449754511	8.527151519	0.020859178
100	2.658981676	2.659203478	0.008340919	0.008340919

Table 7

M	$10^9 U_{300}$ in point B	$10^9 U_{142}$ in point B	ε_1 in point B	ε_2 in point B
50	2.393236558	1.208636561	98.01126618	0.351401094
60	2.397841240	1.519945769	57.75834176	0.159673243
70	2.400094575	1.712669627	40.13762708	0.065849805
80	2.400833450	1.975710565	21.51746782	0.035084831
90	2.401236780	2.208970952	8.703864024	0.018291143
100	2.401451328	2.401676074	0.009357881	0.009357881

Table 8

M	$10^9 U_{300}$ in point D	$10^9 U_{142}$ in point D	ε_1 in point D	ε_2 in point D
50	4.921236855	2.482214775	98.25991304	0.485557091
60	4.930369854	3.162257695	55.91296882	0.300874787
70	4.940368468	3.541921705	39.48271248	0.098688522
80	4.942448468	4.128578203	19.71308826	0.056627949
90	4.943865875	4.566589689	8.261661574	0.027965962
100	4.944736478	4.945248861	0.010361117	0.010361117

Problems for plates with two and three small regions which have different properties were also solved. The obtained accuracy of approximate solutions and the computational time were found to be similar to such parameters for the Problems 1, 2 and are therefore not reported here.

Conclusions

The FEM connected with OFF and corresponding FE models were proved to be effective in plane problems for elastic homogeneous and heterogeneous bodies. This FEM allows obtaining approximate stress-strain state with high accuracy and relatively small computational time without simplification of the structure under consideration and without elimination of its small features. The results of computations illustrate that OFFs allow to improve significantly the characteristics not only of mixed FEMs in elasticity, but also of classical FEMs based on the Lagrange's variational principle, which form the basis of many FE codes, such as ANSYS. These FEs can be used in creating and investigating of heterogeneous materials.

Acknowledgements. *No external funding was received for this study.*

References

[1] Strang G, Fix GJ. *An Analysis of the Finite Element Method.* New Jersey: Prentige-Hall Inc.; 1973.

[2] Daubechies I. Orthonormal bases of compactly supported wavelets. *Comm. Pure and Appl. Math.* 1988;41(7): 909-996.

[3] Leontiev VL. *Ortogonalnie finitnie funksii i chislenie metodi [Orthogonal Finite Functions and Numerical Methods]*. Ulyanovsk: UlSU; 2003. (In Russian)

[4] Ciarlet P. *The Finite Element Method for Elliptic Problems.* Amsterdam: North-Holland Publ. Comp.; 1978.

[5] Rozin LA. *Metod konechnyh elementov v primenenii k uprugim sistemam [FEM in Application to Elastic Systems]*. Moscow: Stroyizdat Publ.; 1977. (In Russian)

[6] Poceski A. A mixed finite element method for bending of plates. *Int. J. Num. Meth. Eng.* 1975;9(1): 3-15.

[7] Poceski A. *Mixed Finite Element Method.* Berlin: Springer; 1992.

[8] Brezzi F, Douglas J, Marini LD. Two Families of Mixed Finite Elements for Second Order Elliptic Problems. *Numer. Math.* 1985;47(2): 217-235.

[9] Boffi D, Brezzi F, Fortin M. *Mixed Finite Element Methods and Applications.* Springer Series in Computational Mathematics. Vol. 44. Berlin: Springer; 2013.

[10] Zienkiewicz OC. *The finite element method in engineering science*. London: McGraw-Hill; 1971.